Bull. Chem. Soc. Ethiop. **2022**, 36(4), 935-948.
DOI: https://dx.doi.org/10.4314/bcse.v36i4.18

ISSN 1011-3924
Printed in Ethiopia
Online ISSN 1726-801X

DETERMINATION OF PARAMETERS AFFECTING KINETIC AND THERMODYNAMIC VALUES FOR LEAD REMOVAL USING WASTEWATER TREATMENT PLANT SEWAGE SLUDGE ASH

Şahset İrdemez[1*], Duygu Yeşilyurt[1], Fatma Ekmekyapar Torun[1] and Sinan Kul[2]

[1]Atatürk University, Environmental Engineering Department, 25240 Erzurum, Turkey
[2]Bayburt University, Department of Emergency Aid and Disaster Management, 69000, Bayburt, Turkey

(Received May 10, 2022; Revised July 6, 2022; Accepted July 7, 2022)

ABSTRACT. In this study, treatment of lead containing wastewater using sewage sludge ash obtained from the incineration unit in the domestic wastewater treatment plant in Gaziantep province in Turkey was investigated. The main purpose of the study is to determine the potential of using the treatment sludge ash, which comes out as waste in the treatment plant, in the treatment of wastewater of another industry. As a result of this study, the most suitable adsorption conditions were determined and focused on the kinetics of adsorption. In the experiments, the lead adsorption capacity of sewage sludge ash was determined as 122 mg g^{-1} at 0.5 g L^{-1} adsorbent concentration in wastewater containing 100 mg L^{-1} Pb^{2+} under optimum conditions. As a result of the research, it was determined that the adsorption reaction proceeds according to the pseudo second degree reaction and is suitable for the Langmuir isotherm. As thermodynamic constants, ΔH° = 7.407 kJ mol^{-1} and ΔS° = 33.25 J mol^{-1} were determined. As a result of this, it was determined that the adsorption reaction was endothermic, spontaneous and random, and adsorption was physical adsorption. The results show that sewage sludge ash can be used in the treatment of water containing high concentrations of Pb^{2+}.

KEY WORDS: Adsorption, Heavy metal, Lead removal, Sewage sludge ash

INTRODUCTION

Heavy metal contamination is a very important problem due to its threat to food safety and its harmful effects on human and animal health [1]. Since there are different definitions in many disciplines, the number of heavy metals may differ [2]. The most widely used definition of heavy metal is elements with a density higher than 5 g cm^{-3} are called heavy metals [3-5]. A total of 53 of the elements in the periodic table are considered to be heavy metals [6]. Heavy metals are among the most important pollutant classes that cannot be decomposed in nature and cause accumulation in the living body [7]. Heavy metals can be directly and indirectly ingested into the human body through inhalation and skin, or through water and food [8, 9]. As a result, heavy metals accumulate rapidly in the blood and in the various organs begin to show toxic effects when they reach a certain concentration [10].

Among heavy metals, lead (Pb) is one of the most hazardous pollutants. Lead is a heavy metal with an atomic number of 82, an atomic weight of 207.2 g mol^{-1} and a density of 11.34 g cm^{-3} [11]. The countries producing the most lead are Germany, USA and Australia [12]. Lead pollution in wastewaters is most common in metal industries, accumulators, battery factories, oil refineries, paint production industries and explosive industries [13]. High lead concentration in the human body causes deterioration in immune, reproductive, kidney and consciousness systems, as well as diseases such as encephalitis, polyneuropathy, hypertension, anemia and cancer [14-17].

Many different methods are used in the treatment of wastewater containing lead and other heavy metals. Chemical precipitation [18], adsorption [19-23], ion exchange [24, 25], reverse osmosis [26] and membrane filtration [27] are the most widely used heavy metal removal

*Corresponding author. E-mail: sirdemez@atauni.edu.tr

methods. However, the adsorption method has been seen as a much more advantageous technique for wastewater containing low concentrations of pollution [28].

The high amount of sludge formed in treatment plants poses an important problem in many countries [29]. Not disposing of sewage sludge affects the environment and causes health problems [30]. The sewage sludge ash (SSA) from incineration facilities is primarily an inorganic and stable material [31, 32]. The SSA predominantly contains silicon oxide and aluminum oxide. The weight ratio of these two compositions in SSA is primarily between 31.5% and 70.8% [33].

This study aimed to remove Pb^{2+} in the waters by adsorption using SSA. The SSA used as adsorbent was obtained from the domestic wastewater treatment plant of Gaziantep Province of Turkey. The adsorbent used has a great advantage because it is a waste that comes out of the biological treatment plant and needs to be removed. In this study, the effects of parameters such as time, pH, temperature, stirring speed, adsorbent, and adsorbate concentration on adsorption were investigated. Isotherm constants and reaction degrees were determined by examining the adsorption kinetics and fitting the results to the isotherm equations. In addition, thermodynamic studies were carried out and the values of thermodynamic parameters were determined. As a result of the characterization studies, the lead removal mechanism was investigated.

EXPERIMENTAL

Materials

SSA used in the experiments was obtained from the incineration unit of the domestic wastewater treatment plant in Gaziantep. This SSA is of basic character and has been pretreated before being used as an adsorbent. The SSA was mixed with HCl acid solution (36.5-38%) in the reactor in such a way that the pH value remained constant at 4.5 and after the pH reached 4.5, it was washed in distilled water (5 times). The washed ash was then dried for 24 hours at 105 °C. The modified SSA was grinded until it reaches a size of fewer than 75 μm.

Methods

Adsorption experiments were carried out in Edmund Buhler GmbH Incubator Hood TH brand shaker. 100 ml wastewaters containing lead were prepared and transferred to 250 ml flasks which are placed into the shaker. After that, samples taken at certain time intervals were filtered through a 0.45 μ membrane filter and analyzed using lead test kits from Merck. The experimental method used in the study is shown schematically in Figure 1.

In adsorption kinetics studies, pseudo-first-order and pseudo-second-order reaction kinetics equations developed for heterogeneous reactions were used to calculate the reaction rate [34-38]. Pseudo first order and pseudo second order reaction kinetics are given in Eqs. (1-2), respectively.

$$\ln(q_e - q_t) = \ln q_e - k_1.t \quad (1)$$

$$\frac{t}{q_t} = \frac{1}{q_e^2.k_2} + \frac{t}{q_e} \quad (2)$$

Here; C_o is initial heavy metal concentration of wastewater (mg L^{-1}), C is heavy metal concentration of the wastewater at time t (mg L^{-1}), q_e given Eq. 3 is the amount of substance adsorbed per unit amount of adsorbent at equilibrium (mg g^{-1}), and q_t given Eq. 4 is the amount of adsorbate adsorbed per unit amount of adsorbent at time t (mg g^{-1}).

$$q_e = \frac{C_0 - C_e}{m} \quad (3)$$

$$q_t = \frac{C_0 - C}{m} \quad (4)$$

Eq. 5 is used to find the Gibbs free energy from the data obtained as a result of experiments at different temperatures.

$$K_c = \frac{C_a}{C_e} \quad (5)$$

Here; K_c is the adsorption equilibrium constant, C_a is amount of substance retained per unit amount of adsorbent (mg g^{-1}), C_e is adsorbate concentration in solution at equilibrium (mg g^{-1}). Eq. 6 is used to calculate the Gibbs free energy [19].

$$\Delta G^o = -R.T.\ln K_c \quad (6)$$

Enthalpy and entropy values can be calculated from Eq. 7.

$$\ln K_c = \frac{\Delta S^o}{R} - \frac{\Delta H^o}{R.T} \quad (7)$$

Freundlich, Langmuir, BET and Temkin isotherm equations were used to determine the equilibrium state between adsorbate and adsorbent at a constant temperature. These isotherm equations are given in Eqs. (8-11), respectively [39-42].

$$\log q_e = \log K_F + \frac{1}{n}.\log C_e \quad (8)$$

$$\frac{1}{q_e} = \frac{1}{a.K_L}.\frac{t}{C_e} + \frac{1}{a} \quad (9)$$

$$\frac{C_e}{(C_s - C_e).q_e} = \frac{1}{K_B.q_s} + \frac{K_B - 1}{K_B.q_s}.\frac{C_e}{C_s} \quad (10)$$

$$q_e = \frac{R.T}{b_T}.\ln K_T + \frac{R.T}{b_T}.\ln C_e;\ B = \frac{R.T}{b_T} \quad (11)$$

Here; K_F (mg g^{-1}) and n (L mg^{-1}) are Freundlich isotherm constants, K_L (L mg^{-1}) and a (mg g^{-1}) are Langmuir isotherm constants, K_B (L mg^{-1}) and q_s (mg g^{-1}) are BET isotherm constants, and b_T (J mol^{-1}) and K_T (L g^{-1}) are Temkin isotherm constants.

Characterization studies

SEM, FT-IR and XRD analyzes were performed to characterize SSA used as an adsorbent. Morphological features of the adsorbents were obtained with a Zeiss Sigma 300 Scanning Electron Microscope. All samples were glued to the sample stub and covered with a 10 nm gold palladium layer for the SEM images. XRD data were obtained using a Bruker D8 Discover XRD device to determine the structural features of adsorbents.

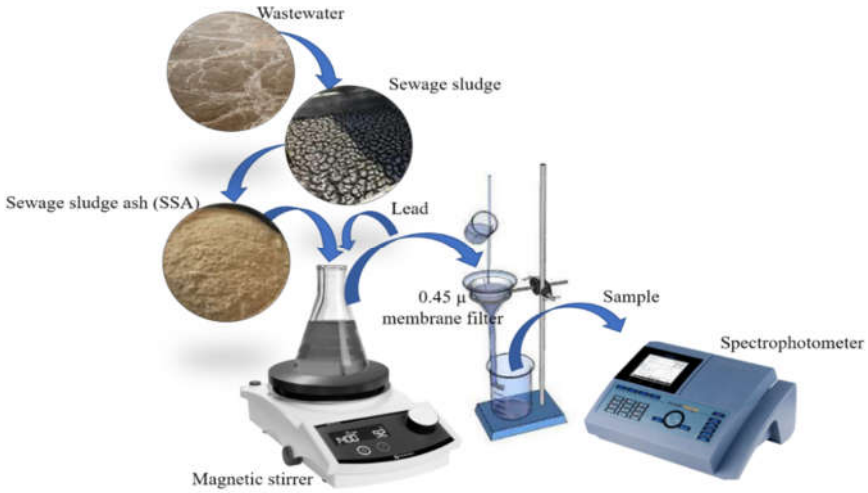

Figure 1. Schematic representation of the experimental method used in the study.

RESULTS AND DISCUSSION

Parameters affecting the adsorption of Pb^{2+}

In the study of removing Pb^{2+} from water by adsorption method using SSA, the effects of initial pH of water, adsorbent concentration, stirring speed and temperature were investigated. The results obtained from the experiments are given in Figure 2. While examining the parameters affecting the adsorption, 100 mg L^{-1} Pb^{2+}, 20 ºC temperature, 200 rpm stirring speed and 0.5 g L^{-1} adsorbent concentration was used except for the parameters examined.

In the Pb^{2+} removal studies using SSA, in the experiments made to examine the effect of pH value on adsorption, pH adjustments were made using 5 N NaOH and 5 N HNO_3. The pH of 100 mg L^{-1} lead solution was determined as 5 and experiments were made by adjusting the pH to 2, 3, 4, 5, and 6. The schematic view of the results obtained is given in Figure 2(a). Since $Pb(OH)_2$ formation pH is above 5.5, it was not possible to determine whether the increase in efficiency above this pH was due to adsorption or chemical precipitation, so pH 5 was chosen as the most appropriate pH. It is seen that the removal efficiencies decrease rapidly especially below pH 3. The reason for this can be thought as that the concentration of H^+ in the environment is very dominant and this decreases the adsorption of Pb^{2+}.

In the Pb^{2+} removal studies where SSA was used as an adsorbent, the experiments made to examine the effect of adsorbent concentration on adsorption were carried out between 0.1 and 10 g L^{-1}. In the experiments, different adsorbent concentrations of SSA were used and the results obtained are shown in Figure 2(b). When the results are examined, the amounts of Pb^{2+} adsorbed per unit adsorbent mass (q_e) in 60 minutes of contact time at adsorbent concentrations of 0.1, 0.5, 1, 3, 5, and 10 gr L^{-1} were determined as 448.5, 72.28, 69.55, 24.4, 15.42, and 8.06 mg g^{-1}, respectively. The experimental results show that increasing the adsorbent concentration increases the adsorption efficiency, but decreases the qe amounts. For this reason, it is important to use the optimum dosage that provides sufficient yield and has sufficient qe values. It can be said that 0.5 g L^{-1} adsorbent concentration is sufficient for 100 mg L^{-1} of Pb^{2+} concentration. Because after this concentration, when the adsorbent dosage is increased 10 and 20 times, the lead removal efficiencies increase by only 9% and 13%, respectively.

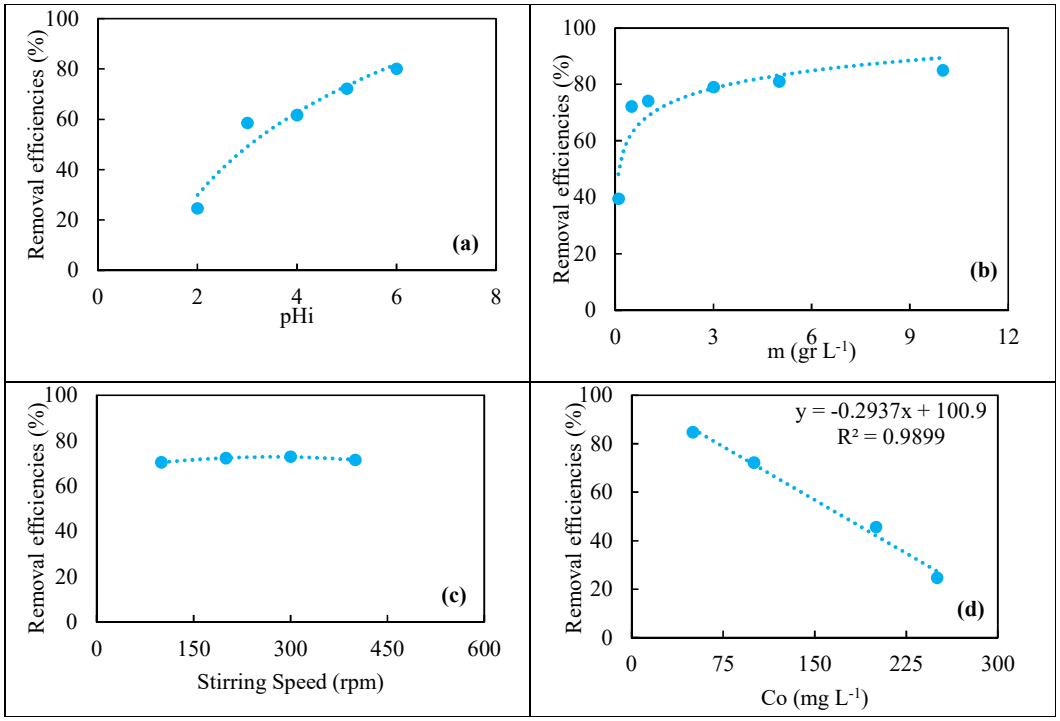

Figure 2. Parameters affecting the removal of Pb^{2+} ions using SSA **(a)** effect of pH, **(b)** effect of adsorbent concentration, **(c)** effect of stirring speed, and **(d)** effect of Pb^{2+} concentration.

Experiments for the effect of stirring speed on adsorption were carried out between 100 and 400 rpm. The results are shown in Figure 2(c). When Figure 2(c) is examined, it is seen that approximately the same efficiencies were obtained for all stirring speeds in 60 minutes. However, the time to reach the equilibrium of adsorption for 100 rpm stirring speed was approximately 45 minutes. The time to equilibrium decreased to 30 minutes at the end of the initial rapid rise at 200 rpm stirring speed. No desorption was observed at 100 and 200 rpm stirring speeds during the experiments. However, at 300 and 400 rpm stirring speeds, the maximum efficiency was reached in the first 5 min, then the desorption and adsorption events followed each other and the removal efficiencies remained approximately constant. For this reason, it was concluded that the stirring speed of 200 rpm is also suitable in terms of energy consumption since desorption does not occur and the contact time is not very long.

When Figure 2(d) is examined, it is seen that the increase in lead concentration decreases the efficiency. Lead removal efficiencies were obtained as 84.8%, 72.73%, 45.6%, and 24.72% for 50, 100, 200, and 250 mg L^{-1} Pb^{2+} concentrations, respectively. The pore diffusion graph drawn using the data obtained in Figure 2(d) is given in Figure 3.

Since a linear trend cannot be obtained in this graph, it can be said that the adsorption is controlled by liquid film diffusion. Since SSA is a multi-component substance, the zeta potential also differs in different regions. In other words, the surface electric charge of SSA can have different charges at different pHs and in different regions. Negative sites on the SSA can attract Pb^{2+}. In this case, the electrostatic attraction provides adsorption [33]. The adsorbent characterization before and after adsorption showed that the concentration of some ions decreased.

In the analysis performed before and after adsorption, the amount of oxygen decreased from 43.84% to 30.32%, and the amount of Ca decreased from 25.36% to 16.36%. This indicates ion exchange adsorption [43]. This shows that the exchangeable cation capacity is an important parameter that affects the adsorption efficiency. The most important evidence of adsorption is that the amount of lead in SSA after adsorption increased to 38.58%.

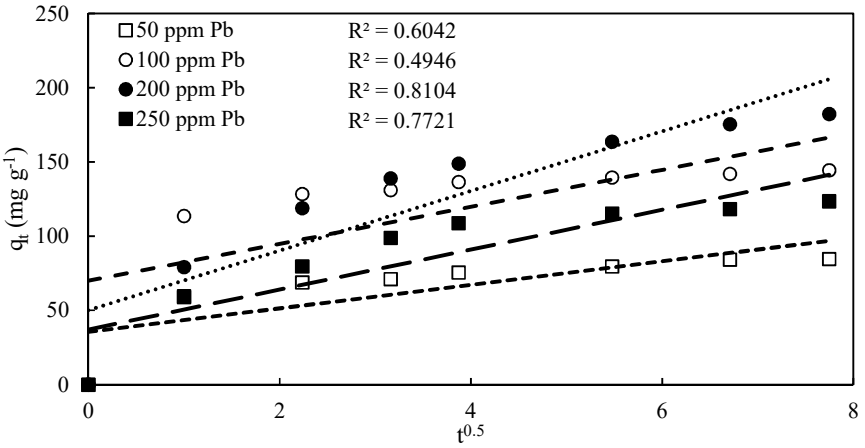

Figure 3. The results of the adsorption experiments performed with different Pb^{2+} concentrations

Effect of temperature

Experiments made to investigate the effect of temperature on adsorption were carried out between 20 °C and 50 °C. The results obtained from the studies conducted at different temperatures are shown in Figure 4.

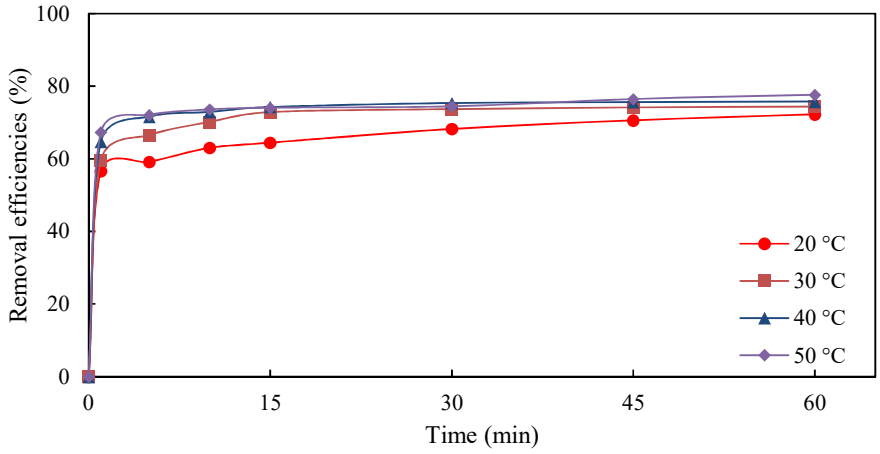

Figure 4. The effect of temperature on lead adsorption using SSA

When Figure 4 is examined, it is seen that temperature has a positive effect on adsorption. However, this effect is very low. While the removal efficiency for 20 ºC was 72.27%, they were

74.41%, 75.83%, and 77.67% for 30 °C, 40 °C, and 50 °C, respectively. Based on these data, after the reaction degree was determined, the activation energy and thermodynamic constants of the reaction were calculated. The results of the adsorption experiments performed with different Pb^{2+} concentrations and the pore diffusion plots are given in Figure 3. The experiments were performed at 20 °C at an adsorbent concentration of 0.5 gr L^{-1} and a stirring speed of 200 rpm.

Repeatability of the experiments

In the studies, 3 different test samples were placed under the same conditions and the arithmetic average of the results obtained was taken. In Table 1, the q_t and standard deviation (SD) values obtained in 3 repetitive experiments with different adsorbent concentrations are given.

Table 1. The q_t and SD values obtained in 3 repetitive experiments with different adsorbent concentrations.

t (min)	m (0.1 g L^{-1})		m (0.5 g L^{-1})		m (1 g L^{-1})		m (3 g L^{-1})		m (5 g L^{-1})		m (10 g L^{-1})	
	q_{ort}	SD	q_{ort}	SD	q_{ort}	SD	q_{ort}	SD	q_{ort}	SD	q_{ort}	SD
0	0.00	0.00	0.00	0.00	0.00	0.00	0.00	0.00	0.00	0.00	0.00	0.00
1	395.60	10.70	95.60	3.30	60.54	2.63	22.16	33.24	13.41	0.41	7.32	0.15
5	425.50	12.20	99.80	4.28	69.55	2.12	25.32	38.32	14.35	0.20	7.47	0.11
10	455.30	17.65	106.40	3.11	72.57	1.24	25.64	40.65	14.68	0.10	7.60	0.11
15	450.80	9.05	108.80	2.69	72.82	1.60	25.70	40.81	15.44	0.27	7.70	0.11
30	464.60	17.47	115.20	3.08	68.54	2.40	24.67	37.99	15.12	0.30	8.00	0.17
45	459.30	9.50	119.20	3.70	68.29	1.78	24.59	37.86	15.29	0.10	8.02	0.02
60	448.50	18.15	122.00	0.87	69.55	1.18	23.87	39.56	15.42	0.03	8.06	0.04

When Table 1 is examined, it is seen that the reproducibility of the experiments is quite high. In particular, the adsorbent behavior obtained in the experiments performed in 3 repetitions shows the same tendency. This is a desirable situation for chemical treatment systems and especially for adsorption.

Adsorption kinetics of Pb^{+2} removal using SSA

Pseudo first order and pseudo second order kinetic graphs were drawn with the data obtained from studies conducted to examine the effect of the amount of adsorbent. The reaction rate constants obtained from these results are shown in Table 2.

Table 2. Reaction rate constants for different adsorbent concentrations for removal of Pb^{2+} using SSA.

Adsorbent concentration (g L^{-1})	$q_{e,\ real}$ (mg g^{-1})	Pseudo first order rate constant (min^{-1})	$q_{e,\ exp}$ (mg g^{-1})	Pseudo second order rate constant (g mg^{-1} min^{-1})	$q_{e,\ exp}$ (mg g^{-1})
0.1	464.6	0.0768	20	0.00736	454
0.5	122	0.0746	38	0.00823	121
1	72.82	0.5085	40	0.104	72.99
3	24.47	0.0375	3.105	0.228	24.57
5	15.42	0.0224	1.47	0.367	15.32
10	8.06	0.0572	1.098	0.485	8.07

When Table 2 is examined, it is seen that the adsorption mechanism of Pb^{2+} removal occurs according to the pseudo second order reaction kinetics. Because both of the results obtained from the experimental data are in accordance with the pseudo second order kinetic equation and the obtained q_e values are closer to the real q_e values.

Adsorption isotherms for Pb^{2+} removal using SSA

The isotherm curves were drawn with the data obtained from the studies to examine the effect of adsorbent concentration, and Freundlich, Langmuir, BET and Temkin isotherms are shown in Figure 5.

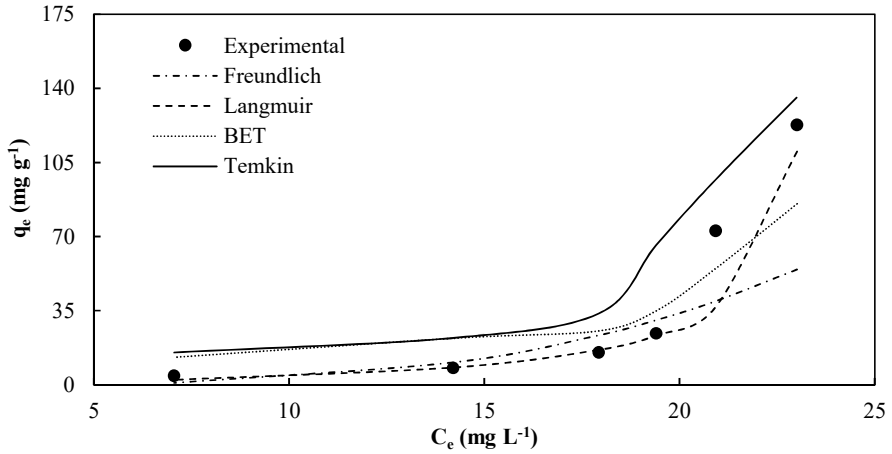

Figure 5. Adsorption isotherm curves for Pb^{2+} removal using SSA.

When Figure 5 is examined, it can be said that the adsorption is more suitable for the Langmuir isotherm than the others. This situation shows that adsorption proceeds in a monolayer and the adsorption rate is directly proportional to the adsorbate concentration and active sites on the surface [40]. The isotherm coefficients calculated with the results obtained from Figure 5 are given in Table 3.

Table 3. Langmuir, Freundlich, BET and Temkin isotherm constants for Pb^{2+} adsorption using SSA at 30 °C.

Langmuir isotherm constants			Freundlich isotherm constants		
K_L	a	R^2	K_F	n	R^2
-0.0413	-5.767	0.9660	$1.36x10^{-3}$	0.296	0.8965
BET isotherm constants			Temkin isotherm constants		
K_B	q_s	R^2	K_T	b_T	R^2
-3.859	$3.36x10^{-3}$	0.9066	0,060	6.001	0.9367

Calculation of the thermodynamic constants in Pb^{2+} removal using SSA

The activation energy of adsorption and other thermodynamic constants were calculated using the results obtained in the experiments conducted to determine the effect of temperature change on the removal of Pb^{2+} using SSA. The data are given in Table 4.

The positive ΔH° value indicates that the reaction is endothermic, and the negative ΔG° value indicates that the adsorption process is spontaneous. The positive ΔS° value indicates that the adsorption process is random [44]. If the activation energy is between 5 kJ mol^{-1} and 40 kJ mol^{-1}, adsorption is defined as physical adsorption [45]. When the activation energy is examined, it shows that adsorption is physical adsorption and occurs rapidly.

Table 4. Activation energy and thermodynamic constants for Pb^{2+} removal using SSA.

T (K)	ΔG° (kJ mol^{-1})	ΔS° (kJ mol^{-1} K^{-1})	ΔH° (kJ mol^{-1})	k_2 (g mg^{-1} min^{-1})	Activation Energy (kJ mol^{-1})
293	-2.334	33.25	7.407	0.0105	28.98
303	-2.600			0.0209	
313	-2.786			0.0296	
323	-3.037			0.0315	

Adsorbent characterization

FT-IR images of SSA before experiments and after lead removal are given in Figure 6(a). When FT-IR graphs are examined, it is seen that the peaks formed at 1008, 1112 and 3605 cm-1 wavelengths before adsorption disappeared after adsorption. The biggest differences between the peaks before and after adsorption are seen as an increase of 9.15% at 598 cm^{-1} and shift of observed peak at 1089 cm^{-1} to 1104 at the end of adsorption and a 10.98% increase of %T. In the 1281-841 cm^{-1} region, the adsorption of sulfate with the stress vibrations of Si-O bonds is observed. O-H bending vibrations of H_2O molecules correspond to bands from 1708 to 1576 cm^{-1}. Stretching vibrations of Fe-O bonds are observed in the 648-515 cm^{-1} region. The overlapping bands in the region from 3660 to 3120 cm^{-1} correspond to the stretching vibrations of Al-OH groups and O-H bonds under hydrogen-bonded groups [46].

The adsorbents that were received before and after the experiments were displayed on the XRD device and the diagram given in Figure 6(b) was obtained. XRD analysis, and samples of SSA by Bruker D8 Discover XRD device were performed on 2ɵ angles in the range 10-90 using 40 mA and 40 kV operating values. When Figure 6(b) is examined, it is seen that sharp peaks have a high degree of the crystalline structure of SSA. In general, it is seen that peaks obtained in two different cases are similar to each other. This demonstrated that chemical reactions between the adsorbent and Pb^{2+} were limited and the adsorption of Pb^{2+} had a negligible effect on the crystal phases of the adsorbent [47].

In the literature, in the characterization studies made with SSA, the basic structure of this substance consists of SiO_2, Al_2O_3, Fe_2O_3, CaO, P_2O_5, SO_3, Na_2O, K_2O, TiO_2, MgO and MnO. The other part is composed of As, Ba, Cd, Co, Cr, Cu, Hg, Ni, Pb, Sn, Sr, V, and Zn at ppm level [48, 49]. However, the content of SSA varies considerably according to the treatment processes used, the type of sludge and the characteristics of the incinerator. While the SSA structure used in this study contains high amounts of Si, Ca, S and O, other substances are present in trace amounts. It was determined that the amount of these substances decreased after adsorption.

While there are high levels of O, Si, Ca and Mg in the SSA, other substances are found in trace amounts. Adsorption of Pb^{2+} on the adsorbent was confirmed by EDX analysis. It was determined that as the Pb^{2+} content on the adsorbent increased, the Ca, Mg, S and O contents decreased. The amount of O, which was 43.84% before the adsorption, decreased to 30.32% after adsorption. The Ca content from 18.61% to 16.36%, the Mg content from 0.75% to 0 decreased. Besides, Pb amount increased from 0 to 38.58%. As can be understood from here, Pb^{2+} bind to instead of SiO_2, MgO and CaO [50].

SEM images magnified by 10000 times are also given in Figure 6(c) and Figure 6(d). SEM results show that SSA had irregular-shaped and porous particles. The micrographs displayed in Figure(c) and Figure 9(d) show a topographic change following adsorption. The surface has formed much denser and much more uniformly stacked crystal phases.

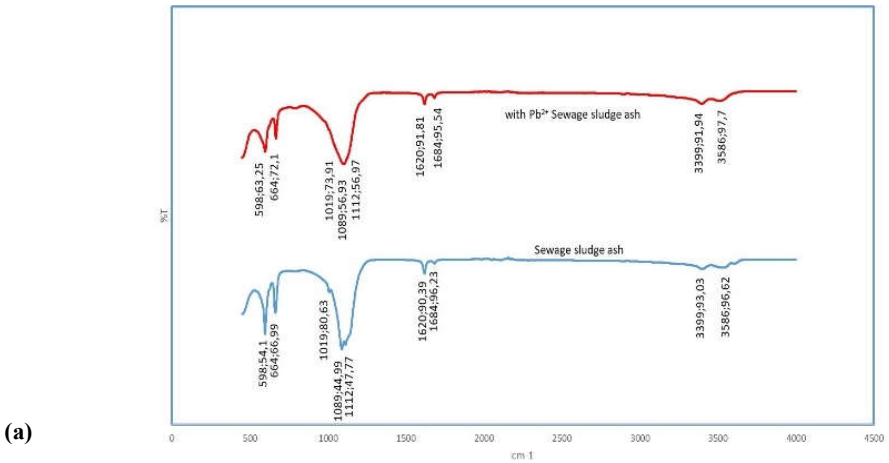

(a)

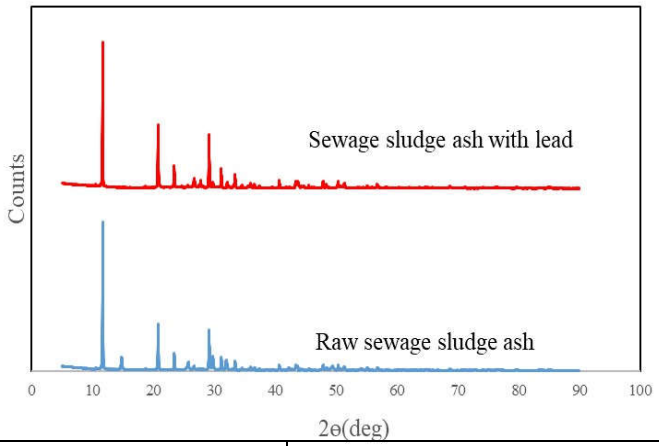

(b)

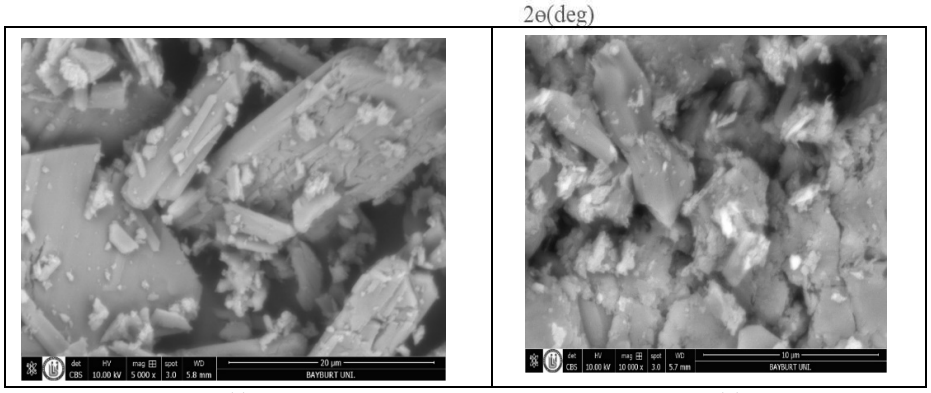

(c) **(d)**

Figure 6. **(a)** FT-IR images of SSA before experiments and after lead removal, **(b)** XRD diagram of SSA before and after adsorption, **(c)** SEM images of SSA before the experiment, and **(d)** SEM images of SSA after lead removal.

CONCLUSIONS

In this study, the parameters effective on adsorption and removal of Pb^{2+} from synthetically prepared wastewater by using ash from the incineration unit of the domestic wastewater treatment plant of Gaziantep were investigated. In the experimental studies, the effects of pH, temperature, stirring speed (rpm) and adsorbent amount (m) on adsorption kinetics were investigated. In the experiments, initial adsorbate concentration was used as 100 mg L^{-1}. The data obtained from the experiments were analyzed according to pseudo-first and pseudo-second-order kinetic models; and the kinetic constants were calculated. In addition, adsorption isotherms were determined from the data obtained. To describe the adsorption reaction, activation energy and thermodynamic constants (enthalpy, entropy and Gibbs free energy values) were calculated.

In studies, the effect of pH has been examined at low pHs. Because, above pH 6, Pb^{+2} combine with hydroxide (OH^-) in water, and precipitate and chemical precipitation occurred instead of adsorption. At the end of the study, they were determined that the most suitable pH values were 5 for Pb^{2+} and other parameters were studied at this pH.

Reaction degree was determined by applying the obtained data to pseudo first and pseudo second order kinetics. As a result of these investigations, it was concluded that the reaction followed the pseudo second degree. According to the pseudo second degree, the reaction rate constant at 20 °C was calculated as 0.0105 g mg^{-1} min^{-1}.

As a result of temperature studies, it was observed that the adsorption rate of Pb^{2+} adsorption increased slightly with the increase of temperature and its efficiency of removal slightly increased. Reaction rate constants, equilibrium constants and activation energy were calculated at the end of the studies to evaluate the effect of temperature. As a result, reaction enthalpy was $\Delta H° = 7.407$ kJ mol^{-1} and reaction entropy was $\Delta S° = 33.25$ kJ mol^{-1} K^{-1} for Pb^{2+} adsorption. If $\Delta H°$ is positive, the reaction is endothermic, and negative $\Delta G°$ indicates that adsorption occurs spontaneously. The positive $\Delta S°$ indicates that the randomness is high. The activation energy of the reaction was calculated as 28.98 kJ mol^{-1} showing that Pb^{2+} adsorption is physical adsorption.

Then, the effect of adsorbent amount for Pb^{2+} adsorption was investigated. Different adsorbent concentrations ranging from 0.1 g L^{-1} to 10 g L^{-1} in the adsorbent dosage in Pb^{2+} removal was studied using 100 mg L^{-1} Pb^{2+}. As a result of the experiments, while Pb^{2+} removal efficiency was 72.27% at 0.5 g L^{-1} adsorbent concentration, the removal efficiency increased to 85.02% when the adsorbent concentration was increased 20 times (10 g L^{-1}).

In the experiments in which the effect of stirring speed was investigated, studies were carried out at 100, 200, 300 and 400 rpm stirring speeds. For Pb^{2+}, the same efficiencies were reached at all stirring speeds, but time to reach equilibrium was shortened as the stirring speed increased. However, desorption was observed at high stirring speeds.

The data obtained as a result of the studies were applied to Freundlich, Langmuir, BET and Temkin isotherms and kinetic constants were calculated for these isotherms. It shows that the adsorption is more suitable for the Langmuir isotherm and that the adsorption proceeds in a single layer and the adsorption rate is directly proportional to the active sites on the surface. Before and after adsorption XRD, SEM and EDX imaging were performed to determine the characterization of SSA. As a result of these, it was determined that SSA has a porous, irregular and high crystal structure.

At the end of this study, it is thought that treatment sludge ash, which is the waste of the treatment plant combustion unit, can be considered quite effective in removing lead.

REFERENCES

1. Hu, B.; Jia, X.; Hu, J.; Xu, D.; Xia, F.; Li, Y. Assessment of heavy metal pollution and health risks in the soil-plant-human system in the Yangtze River Delta, China. *Int. J. Environ. Res.* **2017**, 14, 1042.

2. Ali, H.; Khan, E. What are heavy metals? Long-standing controversy over the scientific use of the term 'heavy metals' – proposal of a comprehensive definition. *Toxicol. Environ. Chem.* **2018**, 100, 6-19.
3. Järup, L. Hazards of heavy metal contamination. *Br. Med. Bull.* **2003**, 68, 167-182.
4. Barakat, M.A. New trends in removing heavy metals from industrial wastewater. *Arab. J. Chem.* **2011**, 4, 361-377.
5. Jaishankar, M.; Tseten, T.; Anbalagan, N.; Mathew, B.B.; Beeregowda, K.N. Toxicity, mechanism and health effects of some heavy metals. *Interdiscip. Toxicol.* **2014**, 7, 60-72.
6. Rahman, Z.; Singh, V.P. The relative impact of toxic heavy metals (THMs) (arsenic (As), cadmium (Cd), chromium (Cr)(VI), mercury (Hg), and lead (Pb)) on the total environment: An overview. *Environ. Monit. Assess.* **2019**, 191, 419.
7. Fu, F.; Wang, Q. Removal of heavy metal ions from wastewaters: A review. *J. Environ. Manage.* **2011**, 92, 407-418.
8. Fu, Z.; Xi, S. The effects of heavy metals on human metabolism. *Toxicol. Mech. Methods.* **2020**, 30, 167-176.
9. Proshad, R.; Islam, S.; Tusher, T.R.; Zhang, D.; Khadka, S.; Gao, J.; Kundu, S. Appraisal of heavy metal toxicity in surface water with human health risk by a novel approach: a study on an urban river in vicinity to industrial areas of Bangladesh. *Toxin Rev.* **2020**, 40, 803-819.
10. Cœurdassier, M.; Vaufleury, A.G.; Lovy, C.; Badot, P.M. Is the cadmium uptake from soil important in bioaccumulation and toxic effects for snails?. *Ecotoxicol. Environ. Saf.* **2002**, 53, 425-431.
11. Aguilar, D.L.G.; Miranda, J.P.R.; Muñoz, J.A.E. Bioadsorption of lead(II) with coffee pulp in synthetic wastewater. *J. Xi'an Univ. Archit. amp; Technol.* **2020**, 12, 1815-1827.
12. Sullivan, M.; Green, D. Toward eliminating children's lead exposure: A comparison of policies and their outcomes in three lead producing and using countries. *Environ. Res. Lett.* **2020**, 15, 103008.
13. Khaoya, S.; Pancharoen, U. Removal of lead(II) from battery industry wastewater by HFSLM. *Int. J. Chem. Eng. Appl.* **2012**, 3, 98-103.
14. Srianujata, S. Lead-the toxic metal to stay with human. *J. Toxicol. Sci.* **1998**, 23, 237-240.
15. Duzgoren-Aydin, N.S. Sources and characteristics of lead pollution in the urban environment of Guangzhou. *Sci. Total Environ.* **2007**, 385, 182-195.
16. Tırınk, S. *Effects of Toxic Heavy Metals on The Environment and Human Health, in Highly Interconnected & Endless Puzzle: Agriculture*, İksad Publishing: Türkiye; **2021**; pp 99-138.
17. Rocha, A.; Trujillo, K.A. Neurotoxicity of low-level lead exposure: History, mechanisms of action, and behavioral effects in humans and preclinical models. *Neurotoxicol.* **2019**, 73, 58-80.
18. Chen, Q.; Yao, Y.; Li, X.; Lu, J.; Zhou, J.; Huang, Z. Comparison of heavy metal removals from aqueous solutions by chemical precipitation and characteristics of precipitates. *J. Water Process. Eng.* **2018**, 26, 289-300.
19. İrdemez, S.; Yeşilyurt, D.; Ekmekyapar Torun, F.; Kul, S.; Bingül, Z. Investigation of manganese ions removal from waters using sewage sludge ash. *Iran. J. Chem. Chem. Eng.* **2021**, DOI: 10.30492/IJCCE.2021.527060.4639.
20. Kul, S. Removal of Cu(II) from aqueous solutions using modified sewage sludge ash. *Int. J. Environ. Sci. Technol.* **2021**, 18, 3795-3806.
21. Meena, A.K.; Mishra, G.K.; Rai, P.K.; Rajagopal, C.; Nagar, P.N. Removal of heavy metal ions from aqueous solutions using carbon aerogel as an adsorbent. *J. Hazard. Mater.* **2005**, 122, 161-170.
22. Nuhoğlu, Y.; Ekmekyapar Kul, Z.; Kul, S.; Nuhoğlu, Ç.; Ekmekyapar Torun, F. Pb(II) biosorption from the aqueous solutions by raw and modified tea factory waste (TFW). *Int. J. Environ. Sci. Technol.* **2021**, 18, 2975-2986.

23. Bingul, Z.; Gurbuz, H.; Aslan, A.; Ercisli, S. Biosorption of zinc(II) from aqueous solutions by nonliving lichen biomass of *Xanthoria parietina* (L.) Th. Fr. *Environ. Eng. Manage. J.* **2016**, 15, 2733-2740.
24. Bashir, A.; Malik, L.A.; Ahad, S.; Manzoor, T.; Bhat, M.A.; Dar, G.N.; Pandih, A.H. Removal of heavy metal ions from aqueous system by ion-exchange and biosorption methods. *Environ. Chem. Lett.* **2019**, 17, 729-754.
25. Koliehova, A.; Trokhymenko, H.; Melnychuk, S.; Gomelya, M. Treatment of wastewater containing a mixture of heavy metal ions (copper-zinc, copper-nickel) using ion-exchange methods. *Ecol. Eng.* **2019**, 20, 146-151.
26. Zhang, H.; Wanga, X.; Li, N.; Xia, J.; Meng, Q.; Ding, J.; Lu, J. Synthesis and characterization of TiO_2/graphene oxide nanocomposites for photoreduction of heavy metal ions in reverse osmosis concentrate. *RSC Adv.* **2018**, 8, 34241-34251.
27. Mukaromah, A.H.; Chasanah, U.; Assyifa, I.R.; Mifbakuddin, Dewi, S.S. Utilization of ZSM-5/TiO_2 powder and membrane to reduce concentration Cu(II) and Cr(VI) ions in water. *Mater. Sci. Eng.* **2020**, 846, 012004.
28. Ali, I.; Gupta, V.K. Advances in water treatment by adsorption technology. *Nat. Protoc.* **2006**, 1, 2661-2667.
29. Pavlík, Z.; Fořt, F.; Záleská, M.; Pavlíková, M.; Trník, A.; Medved, I.; Keppert, M.; Koutsoukos, P.G.; Černý, R. Energy-efficient thermal treatment of sewage sludge for its application in blended cements. *J. Clean. Prod.* **2016**, 12, 409-419.
30. Werther, J.; Ogada, T. Sewage sludge combustion. *Prog. Energy Combust. Sci.* **1999**, 25, 55-116.
31. Lin, K.L.; Chiang, K.Y.; Lin, D.F. Effect of heating temperature on the sintering characteristics of sewage sludge ash. *J. Hazard. Mater.* **2006**, 128, 175-181.
32. Świerczek, L.; Cieślik, B.M.; Konieczka, P. The potential of raw sewage sludge in construction industry – A review. *J. Clean. Prod.* **2018**, 200, 342-356.
33. Pan, S.C.; Lin, C.C.; Tseng, D.H. Reusing sewage sludge ash as adsorbent for copper removal from wastewater. *Resour. Conserv. Recycl.* **2003**, 39, 79-90.
34. Agarwal, S.; Tyagi, I.; Gupta, V.K.; Ghasemi, N.; Shahivand, M.; Ghasemi, M. Kinetics, equilibrium studies and thermodynamics of methylene blue adsorption on Ephedra strobilacea saw dust and modified using phosphoric acid and zinc chloride. *J. Mol. Liq.* **2016**, 218, 208-218.
35. Lagergren, S. Zur theorie der sogenannten adsorption geloster stoffe. *Kungliga Svenska Vetenskapsaakademiens. Handlingar.* **1898**, 24, 1-39.
36. Ho, Y.S. Citation review of Lagergren kinetic rate equation on adsorption reactions. *Scientometrics* **2004**, 59, 171-177.
37. Ho, Y.S.; McKay, G. Sorption of dye from aqueous solution by peat. *Chem. Eng. J.* **1998**, 70, 115-124.
38. Ho, Y.S.; McKay, G. Pseudo-second order model for sorption processes. *Process Biochem.* **1999**, 34, 451-465.
39. Freundlich, H.M.F. Uber die Adsorption in Losungen. *Zeitschrift fr Physikalische Chemie* **1907**, 57, 385-470.
40. Langmuir, I. The adsorption of gases on plane surfaces of glass, mica and platinum. *J. Am. Chem. Soc.* **1918**, 40, 1361-1403.
41. Brunauer, S.; Emmett, P.H.; Teller, E. Adsorption of gases in multimolecular layers. *J. Am. Chem. Soc.* **1938**, 60, 309-319.
42. Temkin, M.; Pyzhev, V. Kinetics of ammonia synthesis on promoted iron catalysts. *Acta Physicochimica URSS* **1940**, 12, 327-356.
43. Wang, F.Y.; Wang, H.; Ma, J.W. Adsorption of cadmium(II) ions from aqueous solution by a new low-cost adsorbent-Bamboo charcoal. *J. Hazard. Mater.* **2010**, 177, 300-306.

44. Lima, E.C.; Hosseini-Bandegharaei, A.; Moreno-Piraján, J.C.; Anastopoulos, I. A critical review of the estimation of the thermodynamic parameters on adsorption equilibria. Wrong use of equilibrium constant in the Van't Hoof equation for calculation of thermodynamic parameters of adsorption. *J. Mol. Liq.* **2019**, 273, 425-434.
45. Wu, C.J. Adsorption of reactive dye onto carbon nanotubes: Equilibrium, kinetics and thermodynamics. *J. Hazard. Mater.* **2007**, 144, 93-100.
46. Chen, P.; Culbreth, M.; Aschner, M. Exposure, epidemiology, and mechanism of the environmental toxicant manganese. *Environ. Sci. Pollut. Res.* **2016**, 23, 13802-13810.
47. Militaru, B.A.; Pode, R.; Lupa, L.; Schmidt, W.; Tekle-Röttering, A.; Kazamer, N. Using sewage sludge ash as an efficient adsorbent for Pb(II) and Cu(II) in single and binary systems. *Molecules* **2020**, 25, 2559.
48. Coutand, M.; Cyr, M.; Clastres, P. Use of sewage sludge ash as mineral admixture in mortars. *Proc. Inst. Civ. Eng.: Constr. Mater.* **2006**, 159, 153-162.
49. Mahieux, P.Y.; Aubert, J.E.; Cyr, M.; Coutand, M.; Husson, B. Quantitative mineralogical composition of complex mineral wastes – Contribution of the Rietveld method. *Waste Manag.* **2010**, 30, 378-388.
50. Wang, Q.; Li, J.S.; Poon, C.S. Using incinerated sewage sludge ash as a high-performance adsorbent for lead removal from aqueous solutions: Performances and mechanisms. *Chemosphere* **2019**, 226, 587-596.